



Oxidation of 2-mercaptopyridine *N*-oxide upon iodine agent: structural and FT-IR studies on charge-assisted hydrogen bonds CAHB(+) and I...I halogen interactions in 2,2'-dithiobis(pyridine *N*-oxide) ionic cocrystal

K. Wzgarda-Raj¹ · A. J. Rybarczyk-Pirek¹ · S. Wojtulewski² · E. Pindelska³ · M. Palusiak¹

Received: 17 December 2018 / Accepted: 16 January 2019 / Published online: 11 March 2019
© The Author(s) 2019

Abstract

2-Mercaptopyridine *N*-oxide (**I**) undergoes spontaneous dimerization to the disulfide form due to reaction with iodine acting as an oxidizing reagent. As a result, a *di-N*-oxide disulfide derivative of pyridine is obtained. During the process of crystallization, one of *N*-oxide groups undergoes protonation and a cation form of disulfide moiety cocrystallizes with I_3^- counterion forming a salt structure. Therefore, in the crystalline state, the 2,2'-dithiobis(pyridine *N*-oxide) molecule exists in a not observed previously form of monocation. Interestingly, the protonated *N*-oxide group does not form hydrogen-bonded salt bridges (of the CAHB(\pm) type with I_3^- anions) but prefers to be involved in intermolecular interactions with the unprotonated *N*-oxide group of the adjacent molecule. This results in formation of intermolecular CAHB(+) hydrogen bridges finally linking molecules into infinite chains. The crystal structure is also stabilized by other various noncovalent interactions, including iodine...iodine and sulfur...iodine contacts.

Keywords Mercaptopyridine *N*-oxide · Pyridinethione · Iodine · Crystal structure · Disulfide · FT-IR studies

Introduction

Chemical derivatives of mercaptopyridine *N*-oxide are known for its diverse biological properties [1, 2]. Among them, the title 2-mercaptopyridine *N*-oxide (1-hydroxy-2(1*H*)-pyridinethione) (**I**) has been proved to be an effective antimicrobial and antifungal agent [3–5] and a potential labelling agent [6]. Mercaptopyridine *N*-oxides are also used as effective ligands in syntheses of transition metal complexes [7–10].

The X-ray studies of the title compound are a part of our ongoing studies on synthesis and analysis of novel pyridine *N*-oxides cocrystals [11–14]. As an object of our work, we have chosen 1-

mercaptopyridine *N*-oxide—a compound of confirmed bioactivity for which two tautomeric forms have been reported [15].

We were interested in obtaining a novel crystal structure stabilized by halogen bonding interactions to *N*-oxide moiety. For this purpose, we have used I_2 iodine as a cocrystallization agent. Hydrogen and halogen bonding interactions responsible for the stabilization of the obtained crystal structure are under our particular attention.

Experimental

Crystallization

Crystals suitable for X-ray measurements were obtained from commercially available reagents (Aldrich Chemical Co.) which were used without further purification. 0.5 mmol of *N*-oxide was mixed with an excess of iodine and dissolved in ethanol (4 mL). The obtained solutions were warmed to 70 °C until dissolution of ingredients and were then kept at room temperature. Crystals (dark brown plates) for X-ray diffraction were obtained after slow evaporation of solvent within 2 weeks.

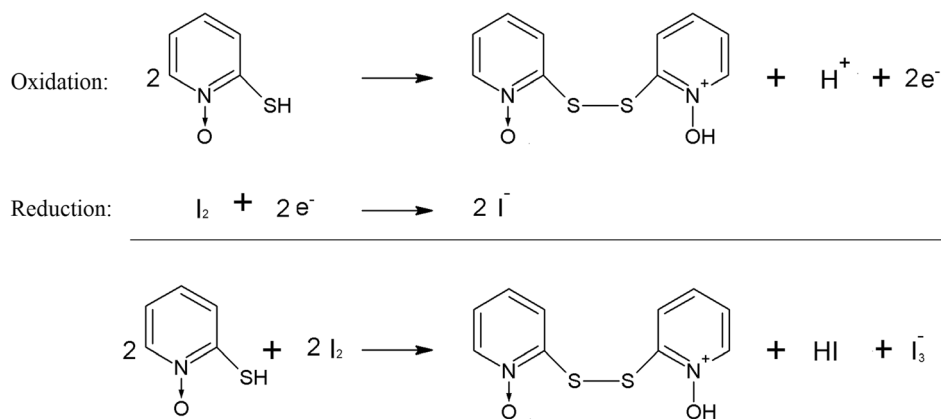
✉ A. J. Rybarczyk-Pirek
agnieszka.rybarczyk@chemia.uni.lodz.pl

¹ Group of Theoretical and Structural Chemistry, Department of Physical Chemistry, Faculty of Chemistry, University of Łódź, Pomorska 163/165, 90-236 Łódź, Poland

² Department of Theoretical Chemistry, University of Białystok, Ciołkowskiego 1K, 15-245 Białystok, Poland

³ Faculty of Pharmacy, Laboratory of Medicine Division, Medical University of Warsaw, Banacha 1, 02-097 Warsaw, Poland

Chart 1 Scheme of redox reaction leading to formation of the final disulfide (II)



X-ray diffraction studies

X-ray data were collected at low temperature (100 K) on Oxford Diffraction SuperNova DualSource diffractometer with monochromated MoK α X-ray source MoK α ($\lambda = 0.71073$). Data reduction and analytical absorption correction were performed with *CrysAlis PRO* [16]. The crystal structure was solved by direct methods in monoclinic $P2_1/c$ space group and refined on F^2 by full-matrix least-squares procedures using *SHELXL-97* [17] ($R [I > 2\sigma(I)] = 0.0156$ and $wR^2 [I > 2\sigma(I)] = 0.0380$). The positions of OH hydrogen atoms were found on a Fourier difference map and refined. Hydrogen atoms of aromatic rings were introduced in calculated positions with idealized geometry and constrained using a rigid body model. Atomic coordinates, displacement parameters, and structure factors of the analyzed crystal structures are deposited with Cambridge Crystallographic Data Centre CCDC (deposit number: 1855702) [18].

Hirshfeld surface analysis

Molecular Hirshfeld surface and fingerprint plots were generated with CrystalExplorer 3.0 [19, 20], using the automatic procedures implemented in the program. The surfaces are mapped with a normalized contact distance (d_{norm}), with values ranging from -0.150 to 1.000 .

Fourier transform infrared spectroscopy (FT-IR) studies

FT-IR analysis was performed with the Perkin Elmer Spectrum 1000 spectrometer. Sample was made into a homogenous mixture in KBr using a mortar and a pestle, then gently pressing the powder under vacuum condition with a compensation force of 10 tons using 14 mm diameter round flat force punch to produce a KBr pellet. Sample was placed in the light path, and the IR spectrum from 400 to 4000 cm^{-1} in transmission mode was obtained (30 scans and with a

2 cm^{-1} resolution). The spectrum was processed using GRAMS/AI 8.0 AI [21].

Results and discussion

X-ray diffraction studies revealed that 2-mercaptopyridine *N*-oxide (I) upon cocrystallization with iodine I_2 undergoes dimerization to the disulfide form [22], that is, in our case, a halfway protonated 2,2'-dithiobis(pyridine *N*-oxide) (II). The unprotonated product of oxidation has been reported in the literature [23, 24] however without detailed description of the reaction scheme. The full scheme of redox reaction with iodine is presented in the Chart 1.

It is clearly seen that, in the investigated case, iodine I_2 acts as a mild oxidation agent leading to the condensation of (I)

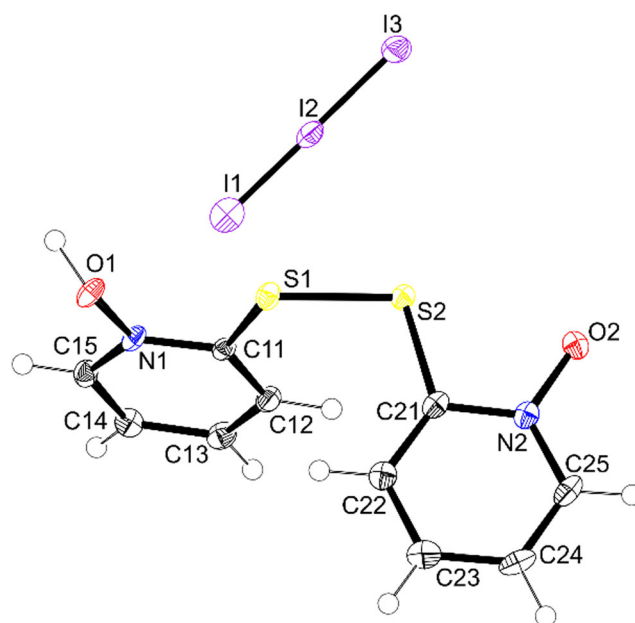
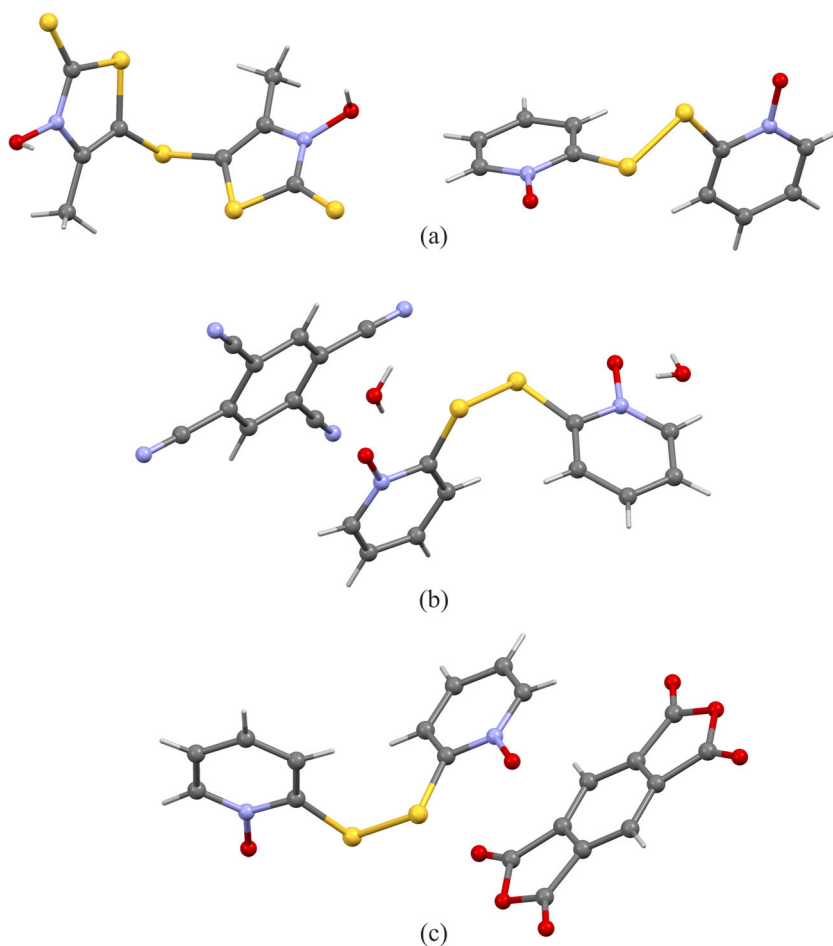


Fig. 1 The molecular structure of 2,2'-dithiobis(pyridine *N*-oxide) (II) cation with I_3^- anion, showing the atom labelling scheme and displacement ellipsoids at 50% probability level

Fig. 2 Cocrystal structures of 2,2'-dithiobis(pyridine *N*-oxide) with corresponding CSD refcodes: 5,5'-thiobis(3-hydroxy-4-methyl-2(3H)-thiazolethione)2,2'-dithiobis(1-hydroxypyridine) (DUDCOU) (a); bis(2,2'-dithiobis(pyridine *N*-oxide)) tetracyanobenzene tetrahydrate (RIRPIR) (b); bis(2,2'-dithiobis(pyridine *N*-oxide)) pyromellitic dianhydride(RIRPOX) (c) [25]



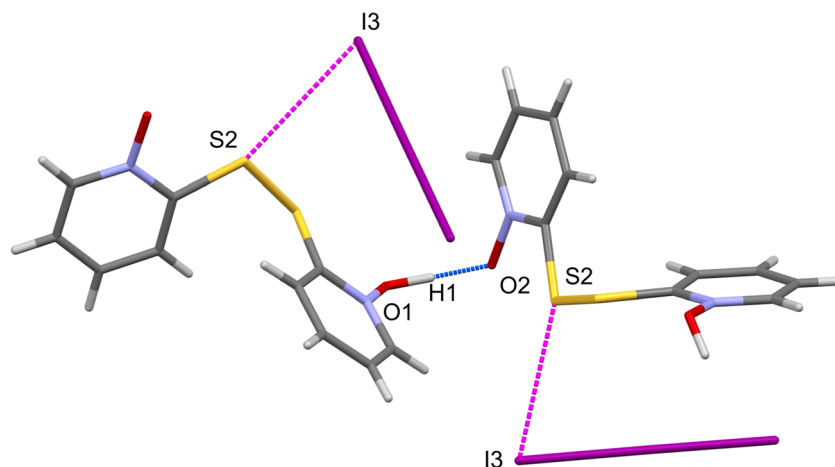
into the disulfide form (**II**) by oxidation of sulfur atoms. The latter one, in the arising acidic environment (formation of HI), exists in partially protonated form (formally one of *N*-oxide groups is protonated). In turn, arising as a result of reduction

reaction, iodide anions Γ^- are bound by iodine molecules forming I_3^- complex anions. The molecular structures of the both disulfide cation molecules (**II**) and I_3^- anions are confirmed by X-ray diffraction studies (see Fig. 1).

Table 1 Comparison of selected bond lengths and angles of 2,2'-dithiobis(pyridine *N*-oxide) molecule [\AA , $^\circ$]

	(II) This work	RIRPIR	RIRPEN	DUDCOU	RIRPOX
Distances					
d (NO)					
N1–O1	1.370(3)	1.318	1.309	1.340	1.318
N2–O2	1.359(3)	1.313	1.316	1.340	1.313
d (SS)					
S1–S2	2.043(9)	2.048	2.054	2.043	2.055
d (CS)					
C11–S1	1.768(3)	1.762	1.767	1.770	1.762
C21–S2	1.771(3)	1.762	1.760	1.770	1.766
d (CN)					
N1–C11	1.355(3)	1.355	1.359	1.337	1.362
N2–C21	1.356(3)	1.357	1.360	1.337	1.365
Angles					
\angle (C11–S1–S2–C21)	–86.10(1)	–87.52	–89.89	–91.47	–92.99

Fig. 3 Scheme of intermolecular interactions O–H...O, I...I and I...S in the title crystal structure



In the crystallization procedure, a novel cocrystal structure of (**II**) has been obtained. Ionization of the hydrogen iodide molecule in ethanol solution is accompanied by a protonation one of *N*-oxide groups. Therefore, in the crystalline state, 2,2'-dithiobis(pyridine *N*-oxide) molecule exists in not observed previously cationic form. Moreover, there is one semiprotonated molecule of (**II**) (cation form) and one I_3^- counter ion in general position of the asymmetric unit ($P2_1/c$ space group). The molecular structure and atomic labelling scheme is presented in Fig. 1.

The unprotonated molecular structure of compound (**II**) is known from other crystallographic studies (CSD refcode RIRPEN) [24]. There are also reported three cocrystal structures: 5,5'-thiobis(3-hydroxy-4-methyl-2(3H)-thiazolethione)2,2'-dithiobis(1-hydroxypyridine) (DUDCOU) [23] (Fig. 2a), bis(2,2'-dithiobis(pyridine *N*-oxide)) tetracyanobenzene tetrahydrate (RIRPIR) [24] (Fig. 2b), and bis(2,2'-dithiobis(pyridine *N*-oxide)) pyromellitic dianhydride (RIRPOX) [18] (Fig. 2c). However, it is worth noting that, to the best of our knowledge, the semiprotonated structure of (**II**) has not been yet observed in the crystalline state [25].

The comparison of selected geometric parameters characterizing 2,2'-dithiobis(pyridine *N*-oxide) molecule known from all the structural X-ray studies is presented in Table 1. Bond lengths of sulfur atoms (SS and CS) in all discussed structures are equal to each other within the experimental errors. Similar situation is observed for CN bonds. However, there is an evident elongation of *N*-oxide NO bonds in (**II**) in comparison with the other crystal structures which results from protonation of the molecule. Localization of hydrogen atom within *N*-oxide...*N*-oxide hydrogen bridge, on the base on difference Fourier map, directly indicates which of the *N*-oxide groups should be treated as a protonated one. Indeed, there are small differences between NO bonds (Table 1), but when 3σ criterion is taken into account, the observed differences are meaningless. This suggests that positive charge in fact involves both *N*-oxide groups but not molecular skeleton. Formally, the observed hydrogen bonding interaction links

cations; however, in practice, only one group (formal donor) is positively charged while the acceptor group retain formally neutral. Taking this fact into account, the observed interaction NO–H⁺...ON could be classified as a positive charge-assisted hydrogen bond CAHB(+) [26].

In the crystal structure, individual molecules of (**II**) are linked with each other by the NO–H⁺...ON hydrogen bonds. These relatively short interactions of the neighboring *N*-oxide groups are responsible for the formation of infinite chains of molecules extending along [010] crystallographic direction (Fig. 3).

The distance between interacting oxygen atoms of donor and acceptor groups O1...O2 is equal 2.416(2) Å and belongs to shortest ones observed in *N*-oxide hydrogen bonds [27–31]. Other geometric parameters of the observed interactions are presented in the Table 2.

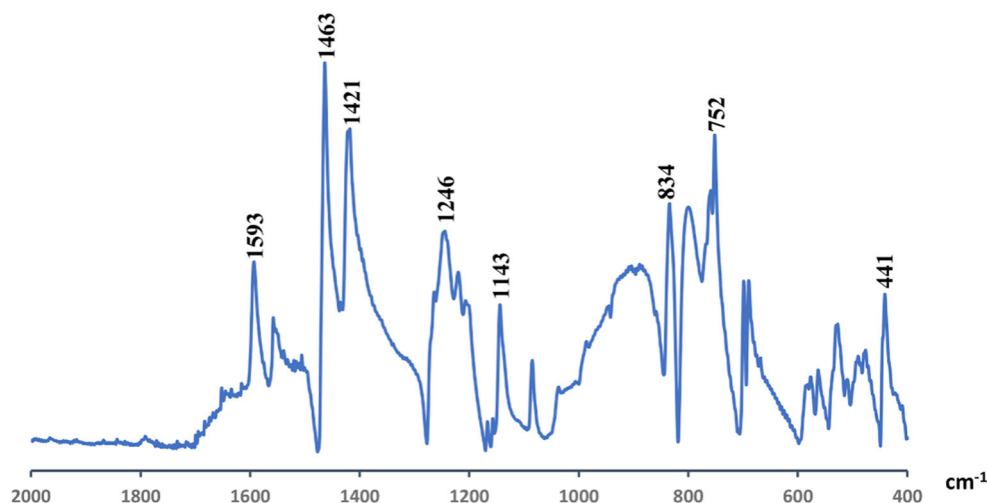
The interesting case of the presented CAHB(+) hydrogen bond has been additionally determined by IR spectroscopic studies. It is rather easy to characterize hydrogen bonding in the solid state by using FT-IR spectroscopic techniques. In the case of the analyzed cocrystal, the stretching vibration of the *N*-oxide N → O moiety (ν_{NO}) is expected to be very sensitive to the state of hydrogen bond. By comparing the 2,2'-dithiobis(pyridine *N*-oxide) spectrum [32] to that recorded on cocrystals of (**II**) (Fig. 4) one can observe expected similarity.

Indeed, ν_{NO} band is seen at 1252 cm⁻¹ in the nonhydrogen-bonded di(2-pyridyl) disulfide S,S'-dioxide

Table 2 Geometric parameters of selected intermolecular interactions

Hydrogen bonds	D–H	H...A	D...A	D–H...A
O1–H1...O2	1.01(3)	1.41(3)	2.416(2)	173(4)
C13–H13...O1	0.95	2.47	3.243(3)	138
C12–H12...O2	0.95	2.56	3.473(3)	161
Iodine interactions			X...Y	X–X...Y
I2–I1...I1			3.697(4)	157.82(1)
I2–I1...I3			4.387(4)	115.71(1)
S2...I3			3.6918(7)	

Fig. 4 FT-IR spectrum of the cocrystal of (**II**)



and at 1246 cm^{-1} in (**II**). However, analyzing the most sensitive spectral region, we can notice main differences by band at 1143 cm^{-1} observed for **II** and not observed for the other case. This band can be assigned to the ν_{NO} mode perturbed by the hydrogen bond interaction, as indicated by X-ray studies. Analogous band shifts in FT-IR spectra were already observed during the proton transfer in pyridine *N*-oxide / acid systems [31].

In the title, cocrystal structure iodide anions I^- are bound to iodine molecules I_2 forming I_3^- complex anions (compare Fig. 1). The bond lengths between iodine atoms in such a complex are of different range while taking into account 3σ criterion. The observed I1–I2 distance is equal to $2.8739(4)\text{ \AA}$ for and $2.9704(4)\text{ \AA}$ for I2–I3 bond. All these three atoms are arranged linearly with I1–I2–I3 angle equal to $179.46(1)^\circ$. Such geometric parameters could indicate predominant covalent character of I1–I2 bond with negative charge accumulated on I3 atom within I_3^- anion.

The structure of anion I_3^- is also known from other crystallographic studies on multicomponent crystals [25]. There is observed similar alternation of I–I bond lengths from $2.7787(6)$ up to $3.0479(8)\text{ \AA}$ with retaining linearity of the molecule [33–35]. Interestingly, the properties of

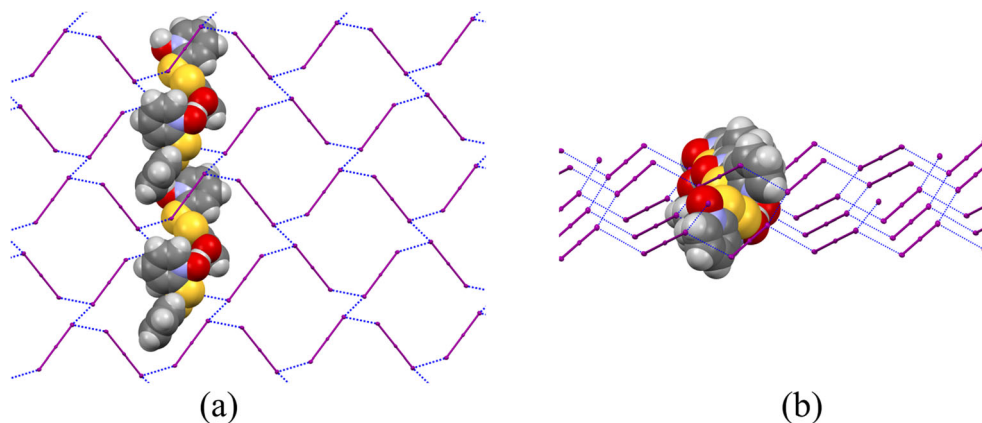
triiodide anion have been also studied by theoretical methods including QTAIM and ELF Theory [35–37].

Interestingly, in the title crystal, as a result of I...I interactions, four I_3^- iodine complex molecules form cyclic structures which includes inside 2,2'-dithiobis(pyridine *N*-oxide) molecules. In turn, these condensed rings form a two-dimensional network of the structure of puckered paper running parallel to (100) lattice plane. Finally, the chains of hydrogen-bonded molecules 2,2'-dithiobis(pyridine *N*-oxide) are intertwined with net built of I_3^- complex molecules of distances close to van der Waals separation (see Fig. 5).

In general, polyiodides, which very often form zigzag chain motives, are unique among halide anions playing the role of supramolecular glue in multicomponent crystals [35, 38].

There are also others intermolecular interactions shorter than the sum of van der Waals radii [39] of the type of C–H...O, I...I and I...S in the title crystal structure. Analysis of molecular Hirshfeld surface indicated that, among all intermolecular contacts of 2,2'-dithiobis(pyridine *N*-oxide) molecule, the most numerous are H...O contacts, with the percentage of 17.5%, resulting from various hydrogen bonds. In turn, for I_3^- anion I...I (of the percentage of 7.9%) and I...S (of the

Fig. 5 The network of I_3^- complex anions intertwined with hydrogen-bonded 2,2'-dithiobis(pyridine *N*-oxide) molecules. View along *a* crystallographic axis (a). View along *b* crystallographic axis (puckered paper structure presented) (b)



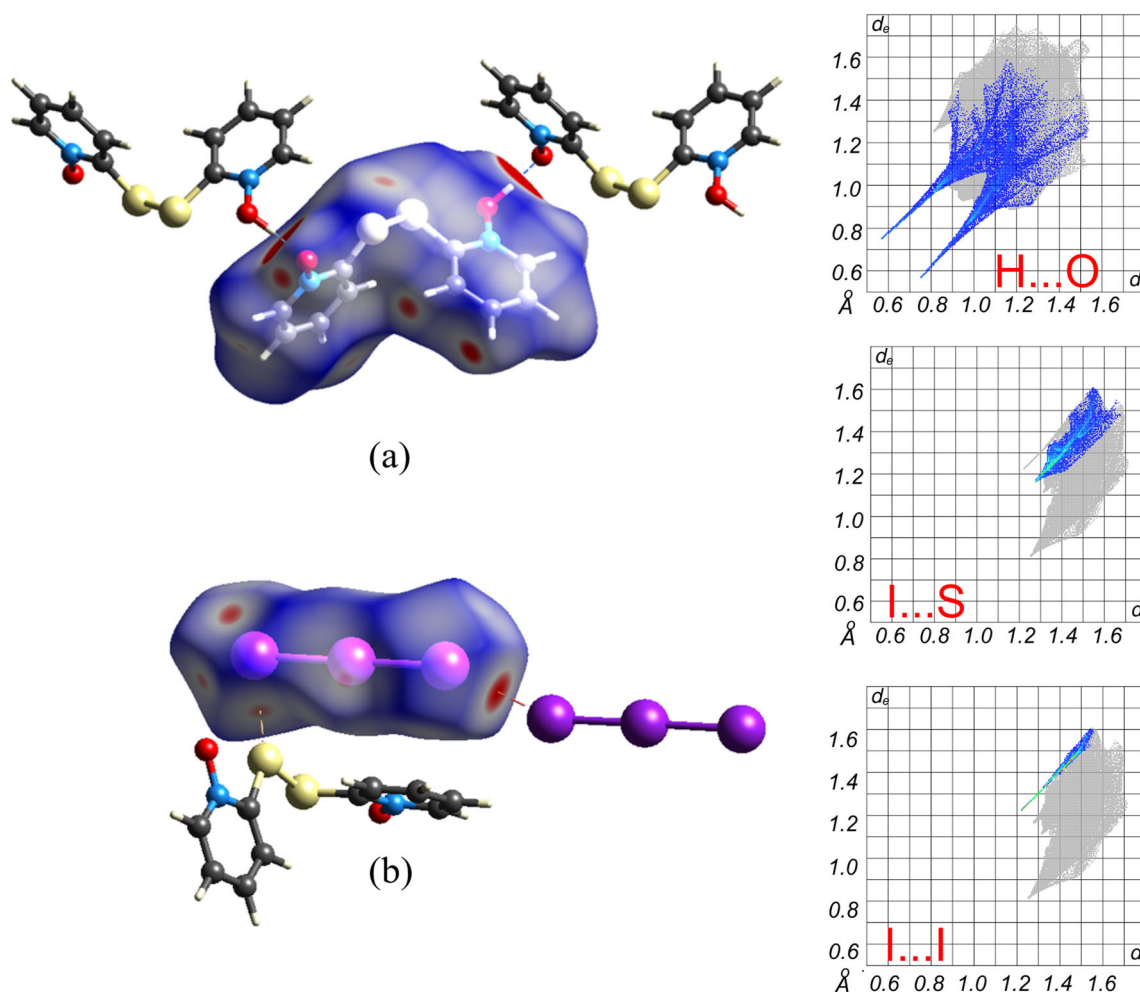


Fig. 6 The molecular Hirshfeld surfaces of 2,2'-dithiobis(pyridine *N*-oxide) (a) and I_3^- iodine complex (b) mapped with the d_{norm} parameter. Red areas resemble intermolecular contacts of distances shorter than van der Waals separation

percentage of 13.9%), contacts are dominant above others. Graphical motifs of the Hirshfeld surface fingerprint plots for selected types of intermolecular interactions are presented in Fig. 6.

Conclusions

We have shown that iodine can be considered a good oxidation agent in the reaction of disulfide bridge formation using a 2-mercaptopyridine *N*-oxide as a starting reagent. During the crystallization process, the final product of reaction undergoes protonation. As a result, one of *N*-oxide groups is protonated while the other one retains in its formally neutral state. Such a half-protonated di-*N*-oxide structure is observed for the first time.

The obtained disulfide cation in solid state forms a salt with I_3^- counterion, as confirmed by X-ray studies and

FT-IR analysis. Interestingly, protonated, that means, formally charged *N*-oxide group which is considered a strong proton donor in potential hydrogen bonding bridges, does not interact with I_3^- anions, which would lead to CAHB(\pm) salt bridges, but prefers to involve the other *N*-oxide group in formation of intermolecular CAHB(+). Other important intermolecular interactions are also present in (II), including iodine...iodine and sulfur...iodine contacts, as depicted by Hirshfeld surface analysis.

Acknowledgements The Oxford Diffraction SuperNova Dual diffractometer was funded by the EFRD in Operational Programme Development of Eastern Poland 2007-2013 via Project no: POPW.01.03.00-20-004/11.

Funding information This research was supported financially by the National Science Centre of Poland (Grant No. 2015/19/ B/ST4/01773). K.W.-R. acknowledges financial support from the Ministry of Science and Higher Education of Poland (designated subsidy for young researchers, University of Lodz project code B1711100001601.02).

Compliance with ethical standards

Conflict of interest The authors declare that they have no competing interests.

Open Access This article is distributed under the terms of the Creative Commons Attribution 4.0 International License (<http://creativecommons.org/licenses/by/4.0/>), which permits unrestricted use, distribution, and reproduction in any medium, provided you give appropriate credit to the original author(s) and the source, provide a link to the Creative Commons license, and indicate if changes were made.

Publisher's Note Springer Nature remains neutral with regard to jurisdictional claims in published maps and institutional affiliations.

References

1. Moe RA, Kirpan J, Linegar CR (1960) *Toxicol Appl Pharmacol* 2:156
2. Delahunt CS, Stebbins RB, Anderson J, Bailey J (1962) *Toxicol Appl Pharmacol* 14:286
3. Scheibel LW, Adler A (1980) *Mol Pharmacol* 18:320
4. Paulus W (1993) *Microbicides for the protection of materials: a handbook*. Chapman and Hall, London, p 294
5. Leonard F, Barkalay FA, Brown EV, Anderson FE, Green DM (1955) *Antibiot Chemother* 6:261
6. Thakur ML, McKenney SL, Park CH (1985) *J Nucl Med* 6:510
7. Davidson JL, Preston PN, Russo MV (1983) *J Chem Soc Dalton Trans* 4:783
8. Boyle TJ, Ottley LAM, Rodriguez MA (2008) *Polyhedron* 27:3079
9. Sanna D, Ugone V, Micera G, Garribata E (2012) *Dalton Trans* 41:7304
10. Hamaguchi T, Kaneko M, Ando I (2013) *Polyhedron* 50:215
11. Rybarczyk-Pirek AJ, Łukomska-Rogala M, Wojtulewski S, Palusiak M (2015) *Cryst Growth Des* 15:5802
12. Łukomska-Rogala M, Rybarczyk-Pirek AJ, Ejsmont K, Jasiński M, Palusiak M (2017) *Struct Chem* 28:1229
13. Wzgarda-Raj K, Rybarczyk-Pirek AJ, Wojtulewski S, Palusiak M (2018) *Acta Crystallogr C* 74:113
14. Rybarczyk-Pirek AJ, Łukomska-Rogala M, Wzgarda-Raj K, Wojtulewski S, Palusiak M (2018) *Cryst Growth Des* 18(12):7373
15. Bond AD, Jones W (1999) *Acta Crystallogr C* 55:1536
16. CrysAlisPRO software system, Oxford Diffraction/Agilent Technologies UK Ltd, Yarnton, England
17. Sheldrick GM (2015) *Acta Crystallogr C* 71:3
18. Cambridge Structural Database Version 5.26., Cambridge Crystallographic Data Centre, 12, Union Road, Cambridge CB2 1EZ, UK
19. McKinnon JJ, Fabbiani FPA, Spackman MA (2007) *Cryst Growth Des* 7:755
20. Spackman MA, Jayatilaka D (2009) *CrystEngComm* 11:19
21. GRAMS/AI 8.0 AI software. Thermo Electron Corp., Waltham
22. Witt D (2008) *Synthesis* 16:2491
23. Bond AD, Jones WJ (2000) *Phys Org Chem* 13:395
24. Bodige SG, Rogers RD, Blackstock SC (1997) *Chem Commun* 17:1669
25. Groom CR, Bruno IJ, Lightfoot MP, Ward SC (2016) *Acta Crystallogr B* 72:171
26. Gilli G, Gilli P (2000) *J Mol Struct* 552:1
27. Wasicki J, Jaskólski M, Pajak Z, Szafran M, Dega-Szafran Z, Adams MA, Parker SF (1999) *J Mol Struct* 476:81
28. Hussain MS, Schlemper EO (1982) *J Chem Soc Dalton Trans* 4:751
29. Song H, Ma B (2007) *Acta Crystallogr E* 63:1332
30. Eichhorn KD (1991) *Z Kristallogr* 195:205
31. Balevicius V, Aidas K, Svoboda I, Fuess H (2012) *J Phys Chem A* 116:8753
32. Kubec R, Krajcowa P, Simek P, Vaclavik L, Hajslova J, Schraml J, Agric J (2011) *Food Chem* 59:5763–5770
33. Marteen L, Wallis JD, Guziak M, Maksymiw P, Konalian-Kempf F, Christian A, Nakatsuji S, Yamada J, Akutsu H (2017) *Dalton Trans* 46:4225–4234
34. Bartashevich EV, Batalov VI, Yushina ID, Stash AI, Chen YS (2016) *Acta Crystallogr C* 72:341–345
35. Bol'shakov OI, Yushina ID, Bartashevich EV, Nelyubina YV, Aysin RR, Rakitin OA (2017) *Struct Chem* 28:1927–1934
36. Lamberts K, Handels P, Englert U, Aubert E, Espinosa E (2016) *CrystEngComm* 18:3832–3841
37. Savastano M, Bazzicalupi C, Garcia C, Gellini C, Lopez de Torre MD, Mariani P, Pichierri F, Bianchi A, Melguizo M (2017) *Dalton Trans* 46:4518–4529
38. Bartashevich EV, Stash AI, Batalov VI, Yushina ID, Drebuschak TN, Boldyreva EV, Tsirelson VG (2016) *Struct Chem* 27:1553–1560
39. Bondi A (1964) *J Phys Chem* 68:441